doi:10.1093/brain/awt299 Brain 2014: 137; 183–196 | 183

BRAIN
A JOURNAL OF NEUROLOGY

Intracranial electroencephalographic seizure-onset patterns: effect of underlying pathology

Piero Perucca, François Dubeau and Jean Gotman

Montreal Neurological Institute and Hospital, McGill University, Montreal, QC, Canada

Correspondence to: Dr. Piero Perucca,
Montreal Neurological Institute,
McGill University,
3801 University Street,
Room 029, Montreal, Québec H3A 2B4, Canada
E-mail: piero.perucca@libero.it

Because seizures originate from different pathological substrates, the question arises of whether distinct or similar mechanisms underlie seizure generation across different pathologies. Better defining intracranial electroencephalographic morphological patterns at seizure-onset could improve the understanding of such mechanisms. To this end, we investigated intracranial electroencephalographic seizure-onset patterns associated with different epileptogenic lesions, and defined high-frequency oscillation correlates of each pattern. We analysed representative seizure types from 33 consecutive patients with drug-resistant focal epilepsy and a structural magnetic resonance imaging lesion (11 mesial temporal sclerosis, nine focal cortical dysplasia, six cortical atrophy, three periventricular nodular heterotopia, three polymicrogyria, and one tuberous sclerosis complex) who underwent depth-electrode electroencephalographic recordings (500 Hz filter, 2000 Hz sampling rate). Patients were included only if seizures arose from contacts located in lesional/peri-lesional tissue, and if clinical manifestations followed the electrographic onset. Seizure-onset patterns were defined independently by two reviewers blinded to clinical information, and consensus was reached after discussion. For each seizure, pre-ictal and ictal sections were selected for high-frequency oscillation analysis. Seven seizure-onset patterns were identified across the 53 seizures sampled: low-voltage fast activity (43%); low-frequency high-amplitude periodic spikes (21%); sharp activity at $\leqslant$13 Hz (15%); spike-and-wave activity (9%); burst of high-amplitude polyspikes (6%); burst suppression (4%); and delta brush (4%). Each pattern occurred across several pathologies, except for periodic spikes, only observed with mesial temporal sclerosis, and delta brush, exclusive to focal cortical dysplasia. However, mesial temporal sclerosis was not always associated with periodic spikes nor focal cortical dysplasia with delta brush. Compared to other patterns, low-voltage fast activity was associated with a larger seizure-onset zone ($P = 0.04$). Four patterns, sharp activity at $\leqslant$13 Hz, low-voltage fast activity, spike-and-wave activity and periodic spikes, were also found in regions of seizure spread, with periodic spikes only emerging from mesial temporal sclerosis. Each of the seven patterns was accompanied by a significant increase in high-frequency oscillations upon seizure-onset. Overall, our data indicate that: (i) biologically-distinct epileptogenic lesions share intracranial electroencephalographic seizure-onset patterns, suggesting that different pathological substrates can affect similarly networks or mechanisms underlying seizure generation; (ii) certain pathologies are associated with intracranial electroencephalographic signatures at seizure-onset, e.g. periodic spikes which may reflect mechanisms specific to mesial temporal sclerosis; (iii) some seizure-onset patterns, including periodic spikes, can also be found in regions of spread, which cautions against relying on the morphology of the initial discharge to define the epileptogenic zone; and (iv) high-frequency oscillations increase at seizure-onset, independently of the pattern.

Keywords: intracranial EEG; seizure-onset; lesional epilepsy; low-voltage fast activity; high-frequency oscillations
Abbreviation: HFO = high frequency oscillation; SOZ = seizure-onset zone

Received April 21, 2013. Revised September 2, 2013. Accepted September 8, 2013. Advance Access publication October 30, 2013

Introduction

Focal epileptic seizures are caused by abnormal or excessive discharges of a localized pool of neurons in the brain (Fisher *et al.*, 2005; Berg *et al.*, 2010). The multifaceted aspects of these discharges can be explored *in vivo* by electroencephalographic recordings with intracranial electrodes (intracranial EEG), which allow direct access to the tissue from which seizures arise. Intracranial EEG patterns at the onset of seizures, in particular, have received considerable attention (Spencer *et al.*, 1992*a*; Spanedda *et al.*, 1997; Lee *et al.*, 2000; Velasco *et al.*, 2000; Wennberg *et al.*, 2002), mainly because of inherent implications for understanding mechanisms of seizure generation (ictogenesis) (Gnatkovsky *et al.*, 2008). Certain patterns have been correlated with the type and degree of underlying neuronal derangements (Williamson *et al.*, 1995; Bragin *et al.*, 2009), whereas others with the intrinsic anatomy or network circuitry in a specific brain region (Spencer *et al.*, 1992*a*; Lee *et al.*, 2000). In addition, intracranial EEG seizure-onset patterns may differ in their ability to guide successful surgical resections (Faught *et al.*, 1992; Bartolomei *et al.*, 2008; Wetjen *et al.*, 2009; David *et al.*, 2011; Dolezalova *et al.*, 2013).

Whether a specific underlying lesion influences seizure-onset patterns is unclear. In mesial temporal lobe epilepsy, an association has been reported between low-frequency high-amplitude periodic spikes (hypersynchronous onset) and neuronal loss and gliosis in the mesial temporal structures, particularly in the hippocampal formation (Spencer *et al.*, 1992*b*; Park *et al.*, 1996; Spanedda *et al.*, 1997; Velasco *et al.*, 2000). In a study in neocortical epilepsy, Lee *et al*. (2000) found that low-voltage fast activity and rhythmic spike-and-wave activity in the alpha-theta range were more common in developmental than in mature pathologies, whereas rhythmic round sinusoidal waves were only expressed in patients with mature aetiologies. Whether differences exist across distinct lesions within each group (developmental or mature pathologies) has not been explored. Similarly, it is unknown whether pathologies other than hippocampal atrophy can generate periodic spikes at the onset of seizures. More generally, it remains unclear whether seizures arising from neurobiologically-distinct epileptogenic lesions differ in their intracranial EEG patterns at seizure-onset.

Another unanswered question is whether different intracranial EEG seizure-onset patterns display distinct profiles of high-frequency oscillations (HFOs), a promising biomarker of epileptogenicity (Zijlmans *et al.*, 2012) that may also be involved in ictogenesis (Bragin *et al.*, 2002; Khosravani *et al.*, 2009). Evidence from animal studies suggests that the two most common patterns in mesial temporal lobe epilepsy, periodic spikes and low-voltage fast activity, may differ in HFO characteristics (Bragin *et al.*, 2005; Lévesque *et al.*, 2012). Specifically, Bragin *et al*. (2005) found a significant increase in ripples and fast ripples at the onset of periodic spikes, without any change in low-voltage fast activity. Lévesque *et al*. (2012) suggested that fast ripples predominate in seizures starting with periodic spikes whereas ripples prevail in those starting with low-voltage fast activity. Whether these findings translate to humans, however, is unclear. Moreover, it is unknown whether other patterns, including those found outside the mesial temporal structures or across different epileptogenic lesions, exhibit specific HFO profiles.

To address these knowledge gaps, we investigated seizure-onset patterns and associated HFO profiles in a large unselected cohort of patients with drug-resistant lesional focal epilepsy undergoing intracranial EEG investigations.

Materials and methods

Patients

Between November 2004 and May 2011, 48 patients with drug-resistant focal epilepsy and a focal structural lesion documented by MRI underwent intracranial EEG monitoring with depth electrodes at a 2000 Hz sampling rate. In all cases, the indication for these investigations was to evaluate the feasibility of epilepsy surgery. From this sample, we included 33 consecutive patients [16 females; median age (range): 30 (16–54) years] with seizures starting in depth electrode contacts located in lesional or peri-lesional tissue (Supplementary Fig. 1). Sixteen patients had malformations of cortical development (nine focal cortical dysplasia; three periventricular nodular heterotopia; three polymicrogyria; one tuberous sclerosis complex), 11 had mesial temporal atrophy/sclerosis, and six had local/regional cortical atrophy. Of note, three patients in the mesial temporal atrophy/sclerosis group had concomitantly extra-temporal local/regional cortical atrophy, from which no seizures were recorded.

This study was approved by the Review Ethics Board (REB) at the Montreal Neurological Institute and Hospital. All patients signed an REB-approved written informed consent.

Magnetic resonance imaging and lesion identification

Pre-implantation MRI images were acquired on a Signa Excite 1.5 T scanner (GE Medical Systems) in 23 patients and on a Tim Trio 3 T scanner (Siemens Medical Solutions) in 10 patients. Sequences included T_1-weighted (with and without gadolinium), T_2-weighted and FLAIR volumes.

Interpretation of MRI images, including lesion identification and definition of lesional borders, was carried out by neuroradiologists experienced in epilepsy imaging.

Intracranial electroencephalogram recordings

Depth electrodes were implanted stereotactically using an image-guided system (SSN Neuronavigation System) (Olivier *et al.*, 1994). In most cases ($n = 27$), implantations consisted of electrodes manufactured on-site (nine contacts, 0.5–1 mm in length and 5 mm apart) (Jirsch *et al.*, 2006). In all other cases ($n = 6$), DIXI Medical electrodes (5–18 contacts, 2 mm in length, and 1.5 mm apart) were used. Epidural electrodes were also placed in a subgroup of 12 patients. Final electrode locations and their relationship with lesional tissue were determined on the post-implantation MRI. Alternatively, these data were obtained by combining the information from the reconstructed position of the electrodes from the Neuronavigation system (Olivier *et al.*, 1994), a post-implantation CT and a post-explantation MRI. Electrode contacts were considered to be in lesional tissue if

located within the visible borders of the lesion, and in peri-lesional tissue if located ⩽1 cm away from the lesional border (Supplementary Fig. 2).

The EEG signal was low-pass filtered at 500 Hz, sampled at 2000 Hz and recorded using the Harmonie monitoring system. Intracranial EEGs were acquired using a referential electrode placed over the parietal lobe contralateral to the suspected epileptogenic zone.

Intracranial electroencephalogram assessment

For each patient, we analysed one representative seizure for each seizure type. Seizure types were defined during the clinical investigation, independently of this study, based on electroclinical characteristics. Seizures with no apparent clinical accompaniment (electrographic seizures) were considered as a separate seizure type. For example, a patient with complex partial seizures and electrographic seizures arising independently from each temporal lobe was considered as having four seizure types. Seizures in which clinical manifestations preceded the electrographic onset were excluded from the analysis.

To ensure that seizure-onset assessment was carried out blindly to patient clinical data, the date, time and any information that could lead to patient identification (name, gender and date of birth) were removed from each intracranial EEG recording and replaced by random numerical codes before review. Concurrent video recording was also removed from each file. The coded intracranial EEGs were then reviewed independently by two neurologists (F.D. and P.P.), who were asked to determine the time and site of seizure-onset, and to describe the morphology of the initial intracranial EEG discharge. For the latter, inter-observer agreement was substantial [Cohen's kappa coefficient = 0.68; 95% confidence interval (CI): 0.53–0.83] (Landis and Koch, 1977); discrepancies were solved after discussion. The seizure-onset was defined as the first unequivocal intracranial EEG sign of change from the background that led to a clear seizure discharge, without return to background activity (first unequivocal ictal intracranial EEG change) (Spanedda *et al*., 1997). The seizure-onset zone (SOZ) was defined as the depth electrode contacts showing the first unequivocal ictal intracranial EEG change. The extent of the SOZ was measured using the ratio between the number of SOZ contacts and the total number of contacts in the brain [$ratio_{(SOZ\ contacts/total\ contacts)}$], to account for interindividual differences in the number of implanted electrodes. A higher $ratio_{(SOZ\ contacts/total\ contacts)}$ is indicative of a larger SOZ. The anatomical location of the SOZ was classified by brain lobe. The temporal lobe was further categorized into mesial and lateral. The time and sites of seizure spread were also assessed. Seizure spread was defined as a clear seizure discharge, starting at least 500 ms after seizure-onset and recorded outside the SOZ. The definition of seizure-onset described above (first unequivocal ictal intracranial EEG change) was also applied to the assessment of the initial discharge in regions of spread.

Three characteristic 4–8 s sections were then selected from the unfiltered intracranial EEG for HFO analysis (Supplementary Fig. 3): background (8 s), ending at least 30 s before the first unequivocal ictal intracranial EEG change; seizure-onset (4–8 s), starting at the first unequivocal ictal intracranial EEG change; and seizure evolution (4–8 s), starting at the earliest intracranial EEG sign of seizure evolution or propagation. The two seizure sections had variable duration to allow the selection of relatively stable ictal intracranial EEG activity (e.g. if a certain pattern evolved into a different activity 5 s after seizure-onset, then the selection of the corresponding section was also halted at 5 s). HFOs were marked in bipolar montage, as described previously (Zijlmans *et al.*, 2009; Jacobs *et al.*, 2010). In brief, the time scale was set to maximal resolution (~0.6 s, 1200 samples). The computer display was split vertically, with an 80 Hz high-pass filter on the left and a 250 Hz high-pass filter on the right, using finite impulse response filters to eliminate ringing. An event was regarded as a ripple if visible on the left (80 Hz) and not on the right (250 Hz), and vice versa, as a fast ripple if visible on the right (250 Hz). Because filtering of sharp transients can result in 'false' HFOs typically consisting of ⩽3 oscillations (Bénar *et al.*, 2010), only discrete events containing ⩾4 consecutive oscillations were considered as HFOs, and two events were regarded as distinct if separated by ⩾2 non-HFO oscillations. To account for event variability in frequency of occurrence and duration, the percentage of time occupied by HFOs in each section (HFO density) was computed for each bipolar contact (Zijlmans *et al.*, 2011).

Analysis strategy

The primary aim of the study was to assess the frequency distribution of each of the identified intracranial EEG seizure-onset patterns across six biologically-distinct epileptogenic lesions: mesial temporal atrophy/sclerosis, focal cortical dysplasia, periventricular nodular heterotopia, polymicrogyria, tuberous sclerosis complex and cortical atrophy.

Additional analyses included: (i) the comparison of the extent of the SOZ across different patterns; (ii) the assessment of whether any of the identified patterns reflected the anatomical location of the SOZ, rather than the underlying pathology; (iii) the comparison of the frequency of each pattern between seizures arising from mesial temporal atrophy/sclerosis and those arising from apparently healthy mesial temporal structures (patients were selected for having seizures starting in structural MRI lesions, but some patients also had seizures starting outside these lesions); (iv) the assessment of whether any of the identified patterns could be detected in regions of seizure spread; and (v) the investigation of pattern-specific changes in HFO density across the three intracranial EEG sections.

Statistical methods

The Fisher's exact test was used for comparisons of categorical data, and the Kruskal-Wallis test or Mann-Whitney U test for comparisons of continuous data. One-way repeated-measures ANOVA was used to assess the time course of changes in HFO density (log-transformed before analysis to approximate normality) in contacts located in lesional/peri-lesional tissue and the SOZ across the three sections, separately for each seizure-onset pattern.

The Bonferroni correction was applied as appropriate to each set of analysis to adjust for multiple comparisons, maintaining the level of significance at 0.05. All analyses were performed with SPSS 19.0 (IBM).

Results

Identification of seizure-onset patterns

From the clinical investigation, it was found that 18 patients had one seizure type, 11 had two seizure types, three had three seizure types, and one had four seizure types. Therefore, 53 seizures [(1 × 18) + (2 × 11) + (3 × 3) + (4 × 1)] arising from lesional/peri-lesional tissue were analysed. Seven intracranial EEG seizure-onset patterns were identified:

(i) Low-voltage fast activity (23 seizures; 18 patients), clearly visible rhythmic activity >13 Hz (Spanedda *et al.*, 1997;

Lee *et al.*, 2000; Wennberg *et al.*, 2002), usually $<10\,\mu V$ in initial amplitude (Faught *et al.*, 1992) (Fig. 1);

(ii) Low-frequency high-amplitude periodic spikes (11 seizures; seven patients), high-voltage spiking at 0.5–2 Hz, lasting >5 s (Spencer *et al.*, 1992*a*; Velasco *et al.*, 2000; Bartolomei *et al.*, 2004) (Fig. 2);

(iii) Sharp activity at $\leqslant 13$ Hz (eight seizures; six patients), low- to medium-voltage sharply-contoured rhythmic activity (Wennberg *et al.*, 2002), most commonly in the alpha-theta range (Spanedda *et al.*, 1997; Schiller *et al.*, 1998) (Fig. 3);

(iv) Spike-and-wave activity (five seizures; five patients), medium- to high-voltage spike-and-wave complexes typically occurring at a frequency of 2–4 Hz (Wennberg *et al.*, 2002) (Fig. 4);

(v) Burst of high-amplitude polyspikes (three seizures; three patients), a single brief burst of repetitive high-voltage spikes (Faught *et al.*, 1992) (Fig. 5);

(vi) Burst suppression (two seizures; two patients), brief bursts of medium- to high-voltage repetitive spikes alternating with brief periods of voltage attenuation (Fig. 6); and

(vii) Delta brush (two seizures; two patients), rhythmic delta waves at 1–2 Hz, with superimposed brief bursts of 20–30 Hz activity overriding each delta wave (Fig. 7). The term 'delta brush' was used because of the resemblance of this pattern to waveforms seen in premature infants (Clancy *et al.*, 2003) and recently also described in patients with anti-NMDA receptor encephalitis (Schmitt *et al.*, 2012).

All seizures displayed a single pattern at seizure-onset, except for one seizure arising from mesial temporal atrophy/sclerosis, which started with two concomitant patterns (low-voltage fast activity in the amygdala and low-frequency high-amplitude periodic spikes in the hippocampus).

To indirectly validate our findings, we compared, in the subgroup of patients undergoing epilepsy surgery ($n = 28$), pattern frequencies between patients who became seizure-free ($n = 9$) and those who did not ($n = 19$), but did not find significant between-group differences (Supplementary Table 1). If it is assumed that removing the SOZ results in seizure-freedom, differences between the two groups would have suggested that certain patterns may reflect seizure spread rather than onset. We also evaluated whether the type of depth electrode used in the intracranial EEG investigation influenced the occurrence of patterns. Of the 53 seizures analysed, 44 were recorded with electrodes manufactured on-site and nine with DIXI electrodes. In the latter group, four patterns were identified [low-voltage fast activity (two seizures), periodic spikes (five seizures), burst of polyspikes (one seizure), and delta brush (one seizure)], each of which was also found in the other larger group. Patterns recorded with DIXI electrodes did not appear different from the same ones recorded with electrodes manufactured on-site.

Considering that we analysed one representative seizure for each of the patients' seizure types (see 'Materials and methods' section), we also assessed whether the pattern found in each of the 53 seizures included in the study was consistent across seizures of the same type, separately for each patient. For 40 of the 53 (75%) seizures included in the study, the pattern analysed was the

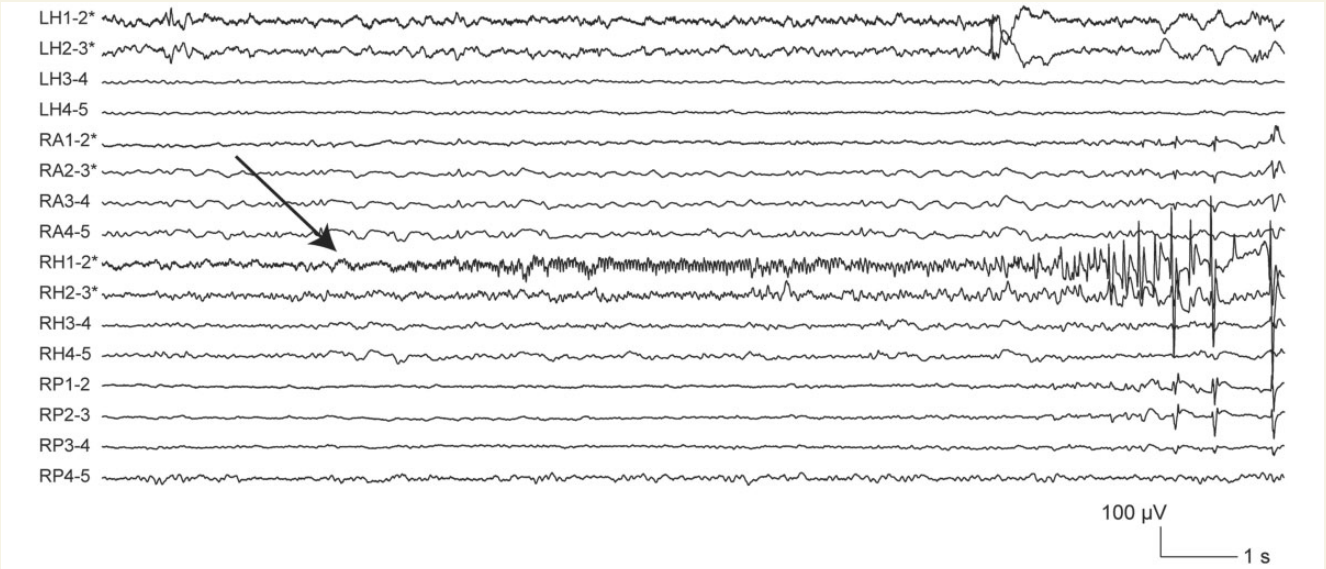

Figure 1 Low-voltage fast activity at seizure-onset. In this ictal intracranial EEG recording (electrographic seizure) from a patient with bilateral mesial temporal atrophy/sclerosis, seizure-onset (arrow) was characterized by a clearly visible rhythmic activity at 20–30 Hz, initially $<10\,\mu V$ in amplitude, which remained confined for several seconds to contacts RH1–2. The patient had seizures arising independently from each mesial temporal lobe, but more frequently from the right side. A right anterior temporal lobectomy was carried out, which resulted in an improvement in the overall seizure frequency, with persistence of seizures only from the left temporal lobe (Engel class III; post-surgical follow-up: 12 months) (Engel *et al.*, 1993). Electrode targets: LH = left hippocampus; RA = right amygdala; RH = right hippocampus; RP = right posterior hippocampus. Asterisk indicates electrode contacts located in lesional/peri-lesional tissue.

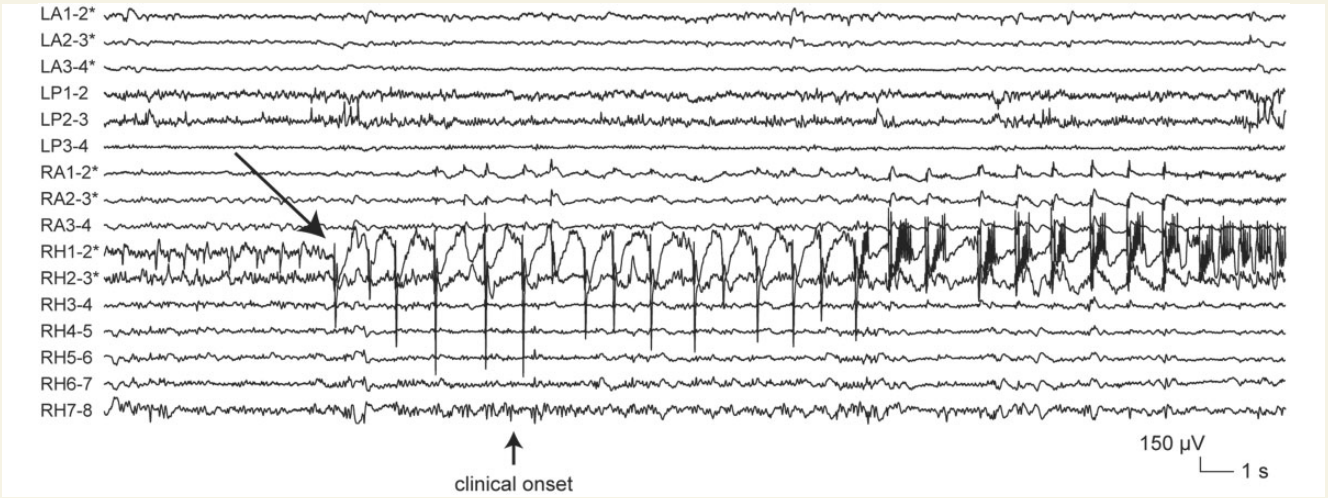

Figure 2 Low-frequency high-amplitude periodic spikes at seizure-onset. In this ictal intracranial EEG recording from a patient with bilateral mesial temporal atrophy/sclerosis (the same described in Fig. 1), seizure-onset (arrow) consisted in the appearance of high-voltage spiking at 1 Hz, lasting for ~15 s at contacts RH1–2. Electrode targets: LA = left amygdala; LP = left posterior hippocampus; RA = right amygdala; RH = right hippocampus. Asterisk indicates electrode contacts located in lesional/perilesional tissue.

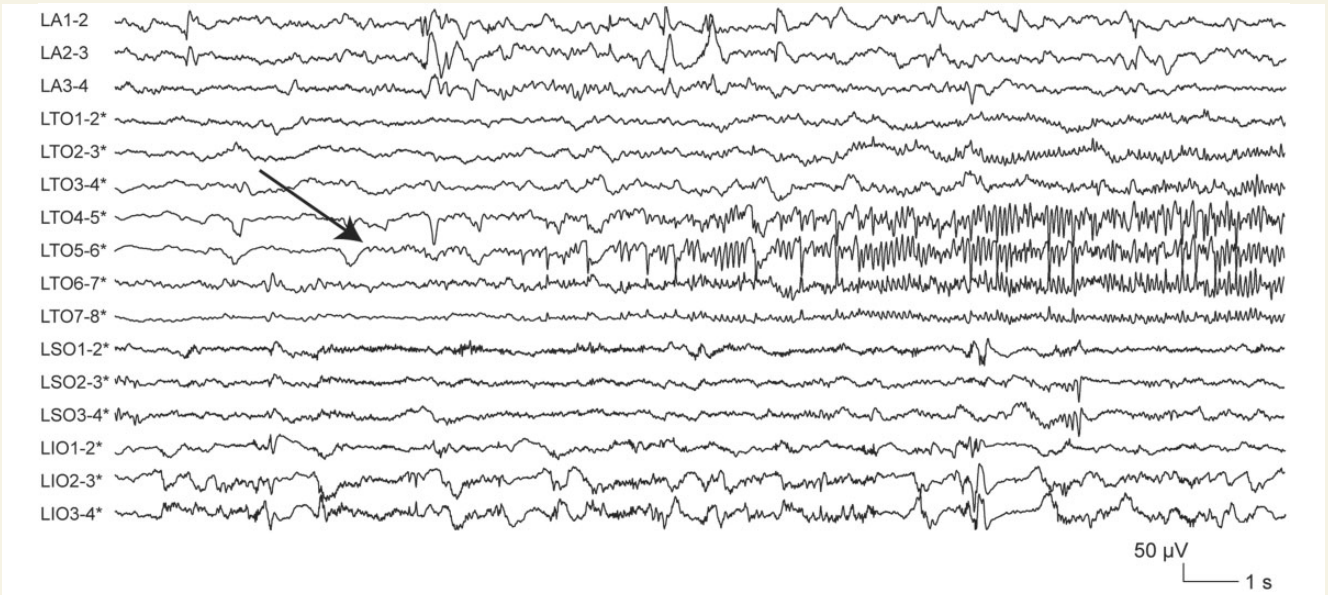

Figure 3 Sharp activity at ⩽13 Hz at seizure-onset. In this ictal intracranial EEG recording (electrographic seizure) from a patient with left temporo-parieto-occipital periventricular nodular heterotopia, seizure-onset (arrow) was characterized by the progressive build-up of a low-to medium-voltage sharply-contoured rhythmic activity at 6 Hz starting at contacts LTO5–6. The patient did not undergo surgery because the epileptogenic lesion was located in close proximity to eloquent cortex (speech area). Electrode targets: LA = left amygdala; LTO = left lingual gyrus; LSO = left precuneus; LIO = left cuneus. Asterisk indicates electrode contacts located in lesional/perilesional tissue.

same across seizures of the same type (median number of seizures/seizure type: 9.5, range: 1–175). For the remaining 13 (25%) seizures included in the study, the pattern analysed was the predominant pattern found across seizures of the same type (median number of seizures/seizure type: 25, range: 2–144).

Distribution of seizure-onset patterns across different pathologies

Most intracranial intracranial EEG seizure-onset patterns (five of seven) were found across multiple epileptogenic lesions (Table 1).

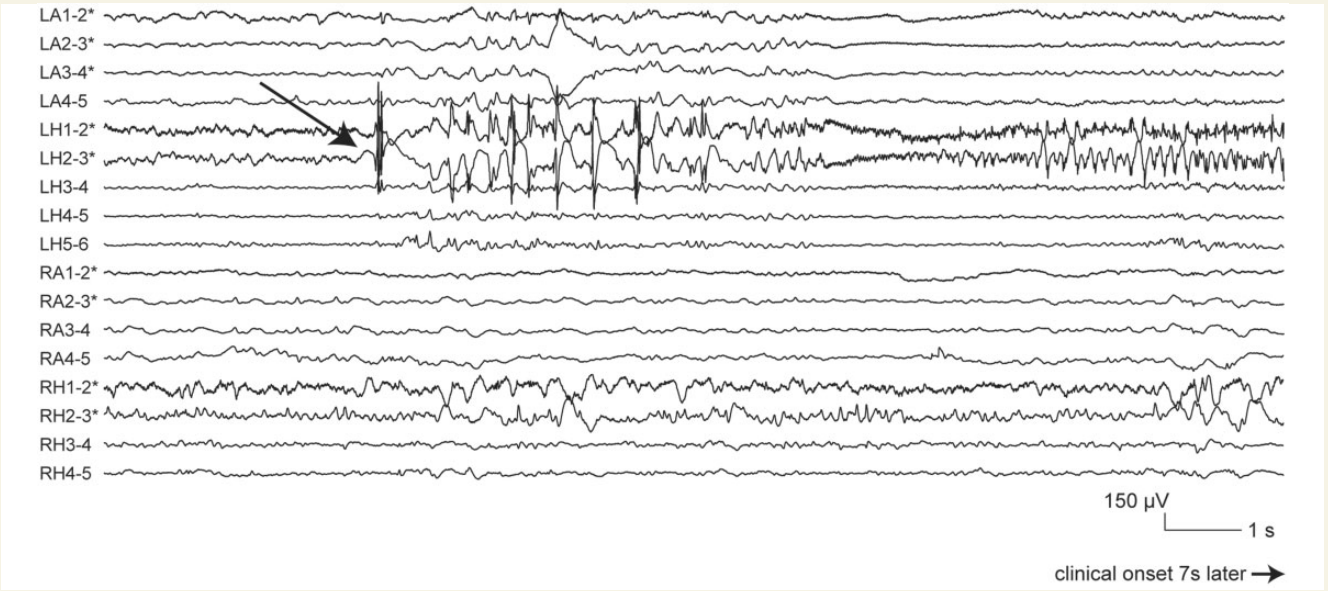

Figure 4 Spike-and-wave activity at seizure-onset. In this ictal intracranial EEG recording from a patient with bilateral mesial temporal atrophy/sclerosis (the same described in Fig. 1), seizure-onset (arrow) consisted in the appearance of high-voltage spike-and-wave complexes at 2–3 Hz at contacts LH1–2 and 2–3. Electrode targets: LA = left amygdala; LP = left posterior hippocampus; RA = right amygdala; RH = right hippocampus. Asterisk indicates electrode contacts located in lesional/perilesional tissue.

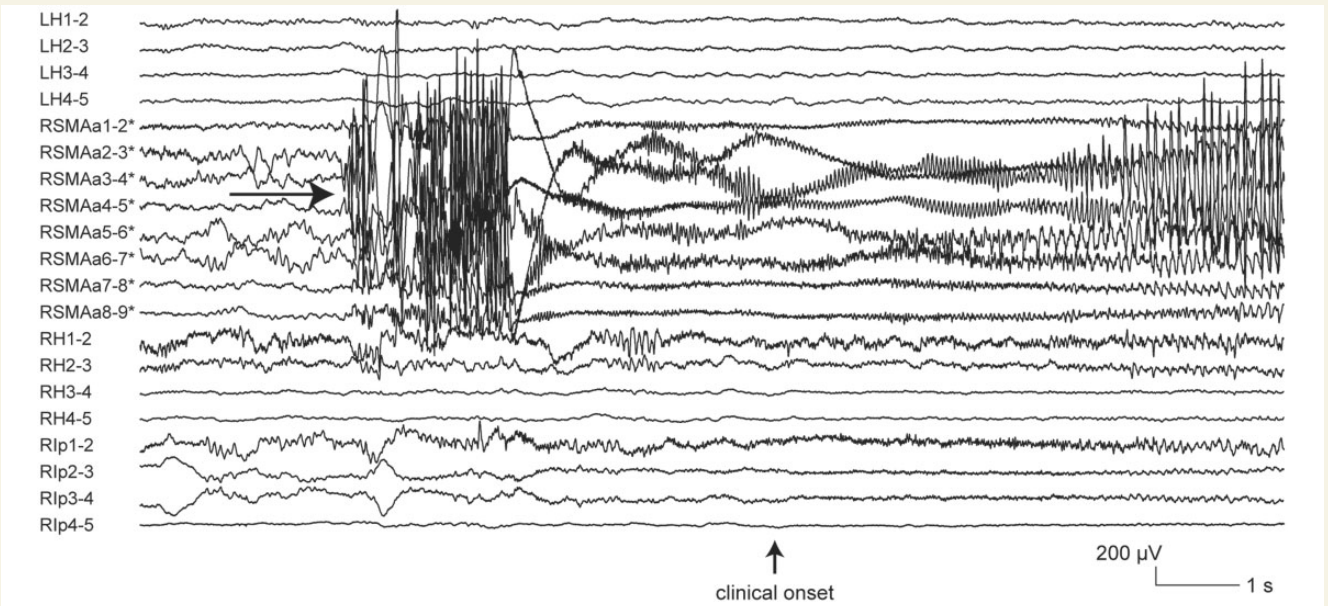

Figure 5 Burst of high-amplitude polyspikes at seizure-onset. In this ictal intracranial EEG recording from a patient with right superior frontal focal cortical dysplasia, seizure-onset (arrow) consisted in a 2-s burst of repetitive high-voltage spikes at all contacts of electrode RSMAa. The patient underwent an incomplete lesionectomy, sparing the portion of the lesion overlapping with the primary motor cortex, with no change in seizure frequency (Engel class IV; post-surgical follow-up: 15 months). Histopathological examination of the resected specimen revealed focal cortical dysplasia type IIa (Blümcke *et al.*, 2011). Electrode targets: LH = left hippocampus; RSMAa = anterior aspect of right supplementary motor area; RH = right hippocampus; RIP = right posterior cingulate gyrus. Asterisk indicates electrode contacts located in lesional/peri-lesional tissue.

Low-voltage fast activity was observed with all lesions, although it was less common in seizures arising from mesial temporal atrophy/sclerosis than those arising from other pathologies (19% versus 59%, $P < 0.05$). For four lesions (focal cortical dysplasia, periventricular nodular heterotopia, polymicrogyria and cortical atrophy), low-voltage fast activity was the predominant pattern (50–80% of all seizures). Sharp activity at $\leqslant$13 Hz was also observed with all lesions except for focal cortical dysplasia. Spike-and-wave

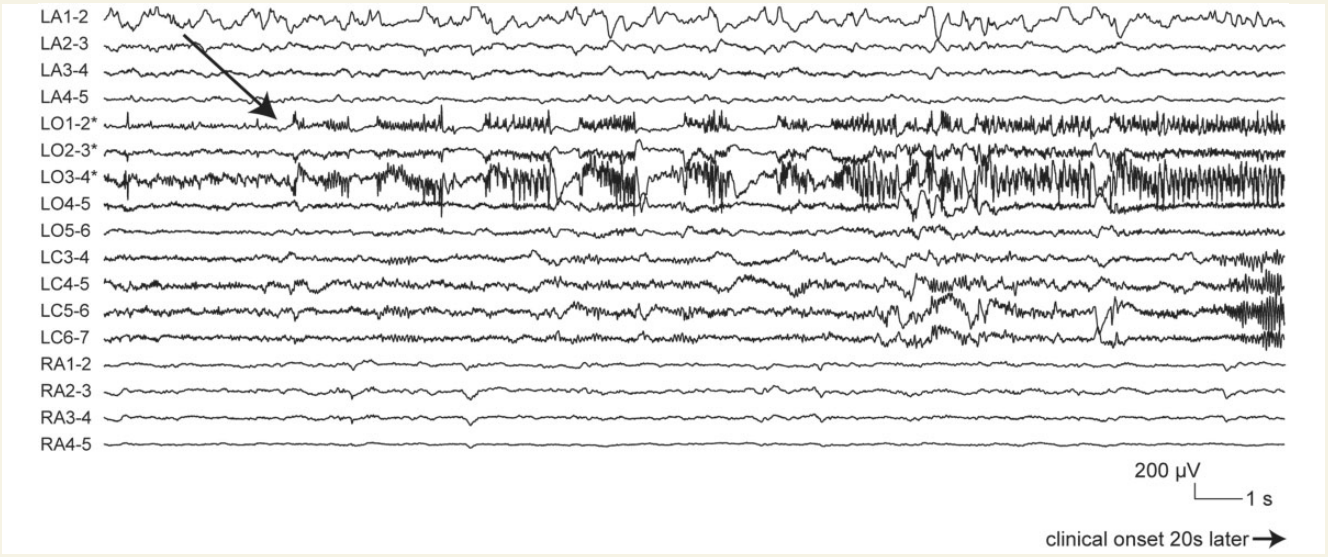

Figure 6 Burst suppression at seizure-onset. In this ictal intracranial EEG recording from a patient with tuberous sclerosis complex, seizure-onset (arrow) was characterized by 1.5-s bursts of medium- to high-voltage polyspikes alternating with 0.5-s periods of voltage attenuation at contacts LO1-2, 2-3 and 3-4. The patient had tubers in both frontal lobes and in the left temporal lobe. Two large tubers, one in the left orbitofrontal region and the other in the left temporal pole, were resected, resulting in a significant improvement in seizure frequency (Engel class III; post-surgical follow-up: 79 months). Electrode targets: LA = left amygdala; LO = left orbitofrontal cortex; LC = left anterior cingulate gyrus; RA = right amygdala. Asterisk indicates electrode contacts located in lesional/peri-lesional tissue.

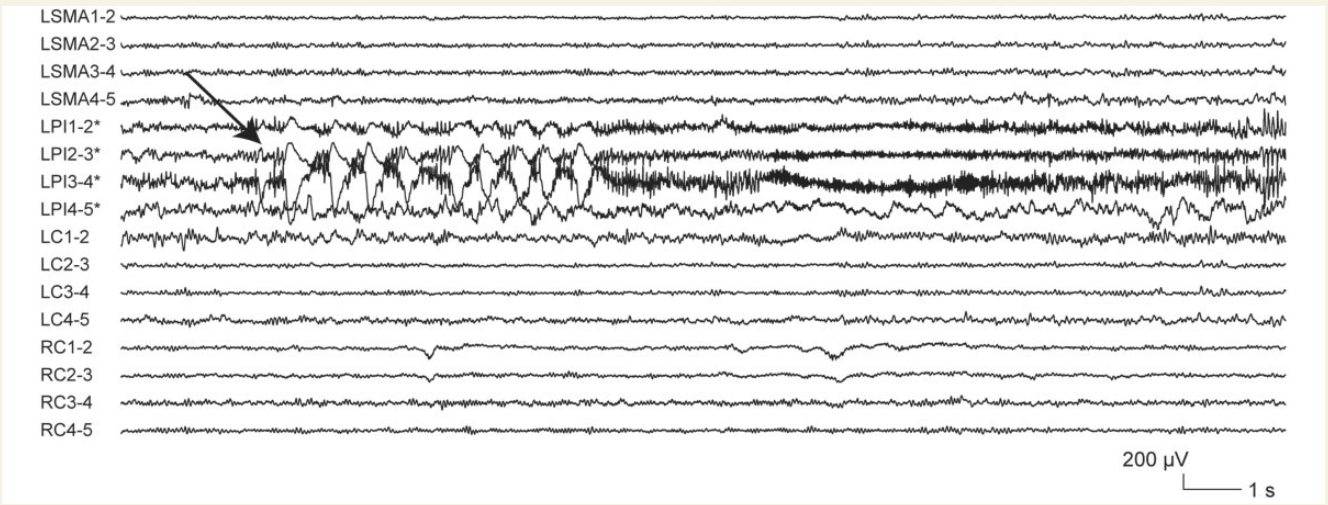

Figure 7 Delta brush at seizure-onset. In this ictal intracranial EEG recording (electrographic seizure) from a patient with left inferior parietal focal cortical dysplasia, seizure-onset (arrow) consisted of the appearance of rhythmic delta waves at 1–2 Hz with superimposed 0.5-s bursts of 20–30 Hz activity at contacts LPI1–2, 2–3 and 3–4. The patient did not undergo surgery because the epileptogenic lesion overlapped with eloquent cortex (speech area). Electrode targets: LSMA = left supplementary motor area; LPI = left infero-parietal region; LC = left anterior cingulate gyrus; RC = right anterior cingulate gyrus. Asterisk indicates electrode contacts located in lesional/perilesional tissue.

activity was found in three lesions, i.e. mesial temporal atrophy/sclerosis, focal cortical dysplasia and cortical atrophy. Burst of high-amplitude polyspikes and burst suppression were each found in two lesions, i.e. focal cortical dysplasia/cortical atrophy and tuberous sclerosis complex/cortical atrophy, respectively.

Two patterns were specific to a single pathology (Table 1). Low-frequency high-amplitude periodic spikes were only observed with mesial temporal atrophy/sclerosis, for which they were the most common pattern (52% of all seizures). Delta brush occurred only in focal cortical dysplasia.

In a separate analysis, we tested whether classifying patterns and pathologies into a smaller number of groups would alter our results (Supplementary Table 2). Patterns were reclassified into four groups: hypersynchronous pattern (corresponding to periodic

Table 1 Distribution of intracranial EEG seizure-onset patterns across different epileptogenic lesions

	Epileptogenic lesions, number of seizures (%)					
	Mesial temporal atrophy/sclerosis	Focal cortical dysplasia	Periventricular nodular heterotopia	Tuberous sclerosis complex	Polymicrogyria	Cortical atrophy
Low-voltage fast activity	4 (19)[a,*]	7 (58)[b]	4 (80)[c]	1 (33)[d]	3 (75)[c]	4 (50)[e]
Low-frequency high-amplitude periodic spikes	11 (52)[f,*]	-	-	-	-	-
Sharp activity at ⩽13 Hz	4 (19)[c]	-	1 (20)[d]	1 (33)[d]	1 (25)[d]	1 (12.5)[d]
Spike-and-wave activity	3 (14)[e]	1 (8)[d]	-	-	-	1 (12.5)[d]
Burst of polyspikes	-	2 (17)[c]	-	-	-	1 (12.5)[d]
Burst suppression	-	-	-	1 (33)[d]	-	1 (12.5)[d]
Delta brush	-	2 (17)[c]	-	-	-	-

Values in cells indicate the number of seizures arising from a certain lesion that displays a specific pattern at onset (% of all seizures arising from that lesion).
[a]From four patients.
[b]From six patients.
[c]From two patients.
[d]From one patient.
[e]From three patients.
[f]From seven patients.
*Concomitant patterns in one seizure.

spikes), fast activity (low-voltage fast activity and sharp activity at ⩽13 Hz); spiking activity (spike-and-wave activity and burst of polyspikes); and burst of fast oscillations (burst suppression and delta brush). Pathologies were reclassified into three groups: mesial temporal atrophy/sclerosis, cortical atrophy and malformations of cortical development (which included focal cortical dysplasia, periventricular nodular heterotopia, tuberous sclerosis complex and polymicrogyria). Notably, this alternative classification scheme confirmed our original results. In fact, most patterns (fast activity, spiking activity and burst of fast oscillations) were again found in multiple pathologies, with their frequency not differing significantly across different lesional groups. The exception was the hypersynchronous pattern, which was specific to mesial temporal atrophy/sclerosis ($P < 0.001$).

Seizure-onset patterns and extent of the seizure-onset zone

The assessment of whether the extent of the SOZ varies across different seizure-onset patterns was limited to patterns occurring in five or more seizures: low-voltage fast activity ($n = 23$), low-frequency high-amplitude periodic spikes ($n = 11$), sharp activity at ⩽ 13 Hz ($n = 8$), and spikes-and-wave activity ($n = 5$).

The median ratio$_{(SOZ\ contacts/total\ contacts)}$, a measure of the extent of the SOZ, differed significantly across the four patterns, being greater in seizures starting with low-voltage fast activity that in those starting with the other three patterns studied ($P = 0.04$, Supplementary Fig. 4).

Seizure-onset patterns and anatomical location of the seizure-onset zone

To determine whether any of the identified patterns reflected the anatomical location of the SOZ, rather than the type of underlying pathology, we assessed the distribution of each pattern across different brain lobes. A pattern found across multiple pathologies, but limited to a single lobe, would indeed suggest an 'anatomical' rather than a 'lesional' origin. For the purpose of this analysis, we analysed only seizures starting in a single lobe ($n = 45$).

Most patterns were observed in multiple lobes (Supplementary Table 3). Low-voltage fast activity and sharp activity at ⩽13 Hz were seen in the frontal, temporal, parietal and occipital lobes. Spike-and-wave activity was recorded in the frontal, temporal and occipital lobes. Delta brush, which in the analysis across lesions was exclusive to focal cortical dysplasia, was found in the frontal and parietal lobes.

Three patterns were limited to a single lobe. Low-frequency high-amplitude periodic spikes, which in the analysis across lesions were specific to mesial temporal atrophy/sclerosis, were recorded only from the mesial temporal lobe. Burst of high-amplitude polyspikes and burst suppression, two infrequent patterns that were shared by multiple lesions, were only observed in the frontal lobe.

Seizure-onset patterns in mesial temporal atrophy/sclerosis versus healthy mesial temporal structures

In addition to the 53 seizures arising from lesional/peri-lesional tissue, there were six seizures in five patients (three with unilateral mesial temporal atrophy/sclerosis and two with polymicrogyria) that started outside the MRI lesion, in apparently healthy mesial temporal structures.

Three seizure-onset patterns were found in these structures: low-voltage fast activity (three seizures; three patients), low-frequency high-amplitude periodic spikes (two seizures; two patients), and sharp activity at ⩽13 Hz (one seizure; one patient). These were also three of the four patterns identified in mesial temporal atrophy/sclerosis (Table 1). There were no significant differences in the frequency of the three patterns between seizures

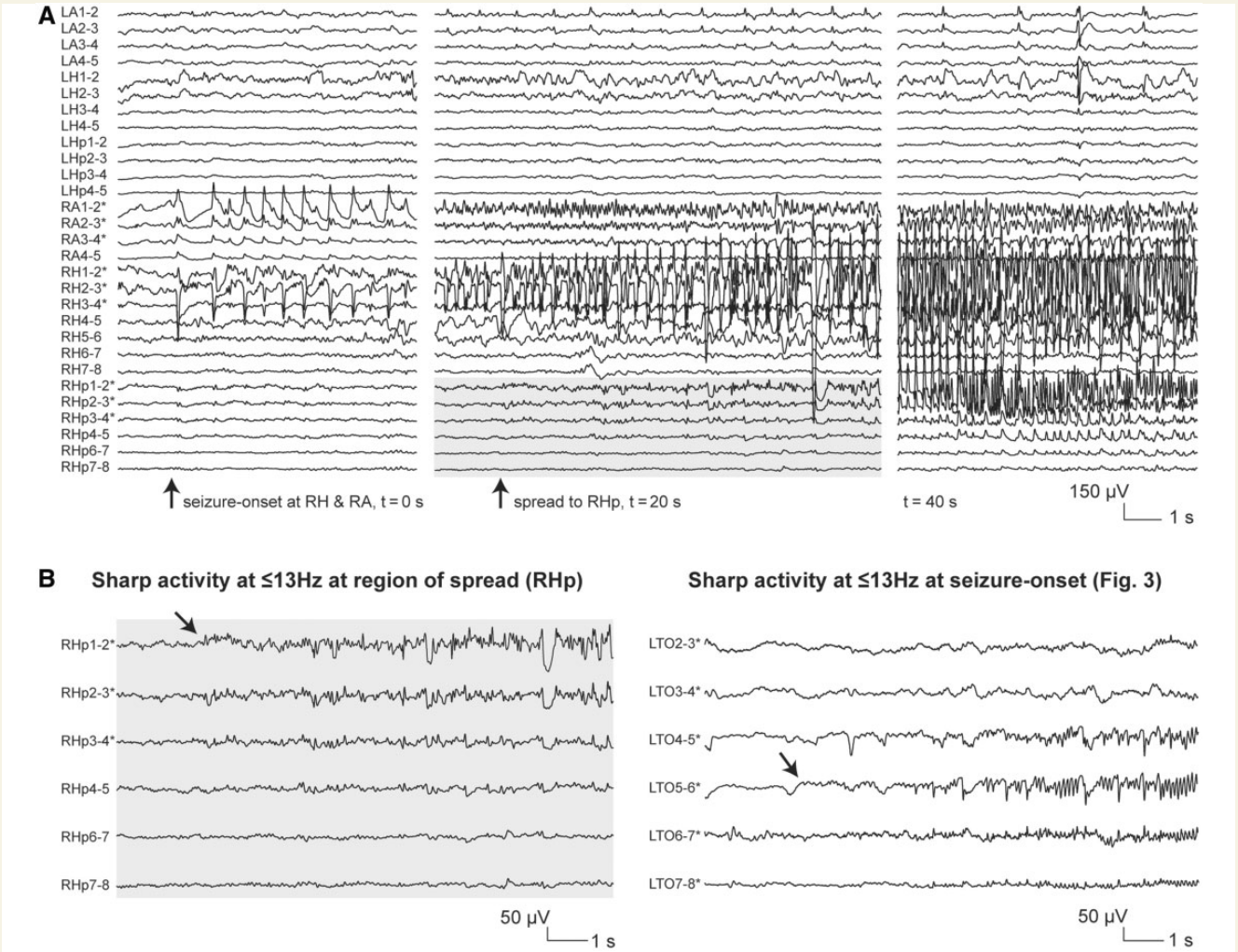

Figure 8 Sharp activity at ⩽13 Hz in a region of seizure spread. (**A**) Ictal intracranial EEG recording (electrographic seizure) from a patient with right mesial temporal atrophy/sclerosis showing seizure-onset at RA1–2 and RH1–2, 2–3 with low-frequency high-amplitude periodic spikes (t = 0 s), followed by seizure spread to right posterior hippocampus starting with the progressive build-up of low- to medium-voltage sharp activity at 9–10 Hz (t = 20 s, grey box), later evolving into high-amplitude rhythmic spiking at 5–6 Hz (t = 40 s). The patient had seizures arising independently from each mesial temporal lobe, but more frequently from the right side. A right anterior temporal lobe resection was performed, with no substantial change in seizure frequency (Engel class IV; post-surgical follow-up: 12 months). (**B**) Comparison of sharp activity at ⩽13 Hz at a region of spread (grey box from **A**) versus seizure-onset (intracranial EEG section excerpted from Fig. 3). Note the similarity of the discharge at the two sites, and, in particular, the fact that there are no features differentiating the site of origin of this pattern. Electrode targets: LA = left amygdala; LH = left hippocampus; LHp = left posterior hippocampus; RA = right amygdala; RH = right hippocampus; RHp = right posterior hippocampus. Asterisk indicates electrode contacts located in lesional/perilesional tissue.

arising from mesial temporal atrophy/sclerosis and those arising from apparently healthy mesial temporal structures.

Identification of seizure-onset patterns in regions of seizure spread

The median time (range) from seizure-onset to the first sign of spread was 5.1 s (500 ms to 102 s). We did not attempt to classify the different intracranial EEG patterns occurring at the time of spread. Instead, we determined if any of the patterns that we defined as seizure-onset patterns were also present at the time of spread. In 51 of 53 seizures analysed (96%), at least one seizure-onset pattern was identified in regions of spread. One pattern was found in 37 seizures, two in 13 seizures, and four in one seizure.

Only four of the seven seizure-onset patterns were detected in regions of spread. Sharp activity at ⩽13 Hz was found in one or more sites of propagation in 30 seizures (Fig. 8), low-voltage fast activity in 24 seizures (Fig. 9), spike-and-wave activity in seven seizures, and low-frequency high-amplitude periodic spikes in six seizures. Sharp activity at ⩽13 Hz and low-voltage fast activity were observed in regions of seizure spread in all epileptogenic lesions, spike-and-wave activity in mesial temporal atrophy/sclerosis and focal cortical dysplasia, and low-frequency high-amplitude

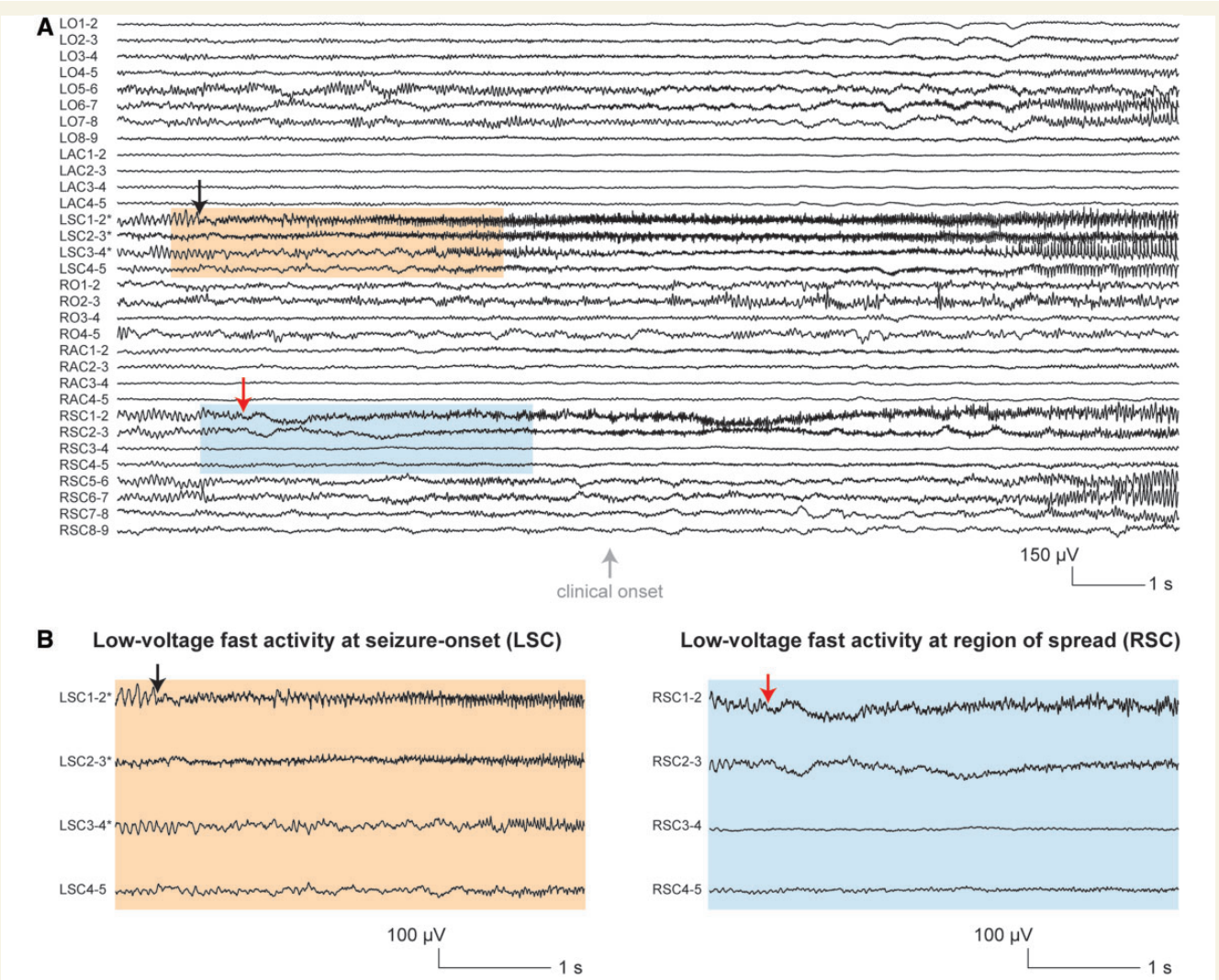

Figure 9 Low-voltage fast activity at the onset of seizure activity in a region of spread. (**A**) Ictal intracranial EEG recording from a patient with left frontal focal cortical dysplasia showing seizure-onset at LSC1–2 with low-voltage fast activity (black arrow), followed by rapid (600 ms) seizure spread to RSC1–2 and 2–3 also starting with low-voltage fast activity (red arrow). The patient underwent a lesionectomy, resulting in a significant improvement in seizure frequency (Engel class III; post-surgical follow-up: 28 months). Histopathological examination of the resected specimen revealed focal cortical dysplasia type IIb (Blümcke *et al.*, 2011). Of note, a post-surgical MRI suggested residual dysplastic tissue along the borders of the surgical cavity. (**B**) Comparison of low-voltage fast activity at seizure-onset (orange box from **A**) versus at a region of spread (blue box from **A**). Note the similarity of the discharge at the two sites, and, in particular, the fact that there are no features differentiating the site of origin of this pattern. Electrode targets: LO = left orbito-frontal cortex; LAC = left anterior cingulate gyrus; LSC = superior aspect of left anterior cingulate gyrus; RO = right orbito-frontal cortex; RAC = right anterior cingulate gyrus; RSC = superior aspect of right anterior cingulate gyrus. Asterisk indicates electrode contacts located in lesional/perilesional tissue.

periodic spikes only in mesial temporal atrophy/sclerosis (Table 2). Of note, periodic spikes were only seen in mesial temporal structures, because of propagation of the same pattern within the hippocampus (e.g. from the anterior to the posterior hippocampus) or from the hippocampus to the ipsilateral amygdala.

In seizures with a focal SOZ (one to four contacts of one electrode or two adjacent electrodes; Lee *et al.*, 2000), we also evaluated whether early spread (i.e. in the first second after seizure-onset) to neighbouring regions emerged with a pattern different from that seen at onset. Detecting differences would argue against the reliability of seizure-onset patterns, particularly if contacts were placed only in close vicinity to the SOZ. Of 35 seizures with a focal SOZ, 16 had early spread to neighbouring regions. In all but two cases, the pattern in neighbouring regions was the same as the one found at onset.

Seizure-onset patterns and high-frequency oscillations

In each seizure-onset pattern, HFO density was found to increase significantly across the three sections (Fig. 10). This finding was largely attributable to a significant increase in HFO density from

Table 2 Frequency of occurrence of intracranial EEG seizure-onset patterns in regions of spread, stratified by pathology

	Epileptogenic lesions, number of seizures (%)					
	Mesial temporal atrophy/sclerosis	Focal cortical dysplasia	Periventricular nodular heterotopia	Tuberous sclerosis complex	Polymicrogyria	Cortical atrophy
Low-voltage fast activity	6 (29)[a]	7 (58)[b]	3 (60)[c]	3 (100)[c]	2 (50)[c]	3 (37.5)[d]
Low-frequency high-amplitude periodic spikes	6 (29)[a]	-	-	-	-	-
Sharp activity at ⩽13 Hz	11 (52)[e]	5 (42)[b]	5 (100)[f]	2 (67)[c]	2 (50)[d]	5 (62.5)[a]
Spike-and-wave activity	5 (24)[f]	2 (17)[c]	-	-	-	-

Only four of the seven seizure-onset patterns (low-voltage fast activity, low-frequency high-amplitude periodic spikes, sharp activity at ⩽13 Hz, and spike-and-wave activity) were found in regions of spread. Values in cells indicate the number of seizures arising from a certain lesion that displays a specific pattern at one or more sites of propagation (% of all seizures arising from that lesion). In 12 seizures multiple patterns were found at sites of propagation.
[a]From four patients.
[b]From five patients.
[c]From one patient.
[d]From two patients.
[e]From eight patients.
[f]From three patients.

the background to the seizure-onset section, a finding that applied to both ripples and fast ripples in four patterns (low-voltage fast activity, low-frequency high-amplitude periodic spikes, burst of high-amplitude polyspikes, and delta brush) and to ripples only in the remaining three patterns (sharp activity at ⩽13 Hz, spike-and-wave activity, and burst suppression).

In most patterns, there were no significant differences in HFO density between the seizure-onset and seizure evolution section (Fig. 10). In low-voltage fast activity, however, ripple density was found to decrease after seizure-onset ($P < 0.05$). In periodic spikes and spike-and-wave activity, ripple and fast ripple densities continued to increase after seizure-onset (all $P < 0.05$).

Discussion

This is the first study characterizing intracranial EEG seizure-onset patterns across different epileptogenic lesions. In a sizeable cohort of consecutive patients with seizures arising from a MRI-documented structural lesion, including mesial temporal atrophy/sclerosis, focal cortical dysplasia, periventricular nodular heterotopia, tuberous sclerosis complex, polymicrogyria, and cortical atrophy, seven distinct morphological patterns could be identified at seizure-onset: low-voltage fast activity, low-frequency high-amplitude periodic spikes, sharp activity at ⩽13 Hz, spike-and-wave activity, burst of polyspikes, burst suppression and delta brush. Remarkably, with the exception of periodic spikes and delta brush, each pattern was shared by two or more lesions, with low-voltage fast activity, the most common pattern, being observed across all pathologies. Overall, these findings are consistent with the hypothesis that different epileptogenic lesions can similarly affect networks or mechanisms underlying seizure generation.

This hypothesis is supported by converging lines of evidence. In experimental models of epileptogenesis, different brain insults, such as status epilepticus, traumatic brain injury and stroke, can induce similar alterations in cellular connectivity and molecular pathways before occurrence of the first seizure (Pitkänen *et al.*, 2007; Pitkänen and Lukasiuk, 2011). An *ad hoc* example is the mammalian target of rapamycin (mTOR) signalling cascade, which is disrupted in models of tuberous sclerosis complex, mesial temporal atrophy/sclerosis, hypoxia and traumatic brain injury, and has recently attracted interest as a potential target for anti-epileptogenic interventions (Galanopoulou *et al.*, 2012; Vezzani, 2012). The hypothesis that different pathologies can similarly impact on underpinnings of focal seizure generation is also consistent with the observation that the efficacy of anti-seizure drugs used in the treatment of focal seizures is not limited to patients with a specific type of epileptogenic lesion (Mohanraj and Brodie, 2005).

Two seizure-onset patterns, low-frequency high-amplitude periodic spikes and delta brush, were not shared by multiple pathologies. Periodic spikes were found only in mesial temporal atrophy/sclerosis, in which they were also the most common pattern (52% of mesial temporal atrophy/sclerosis seizures). This finding was reinforced by the analysis of whether seizure-onset patterns were also present in regions of spread, which revealed that periodic spikes can emerge at the time of propagation, but exclusively from mesial temporal atrophy/sclerosis. In a comparative assessment of seizure-onset patterns in lesional versus non-lesional mesial temporal structures, periodic spikes were slightly more common among seizures arising from mesial temporal atrophy/sclerosis than among those starting from an apparently healthy hippocampus and/or amygdala (52% versus 33%), but numbers were too small to detect significant differences. Moreover, it cannot be excluded that the two seizures starting with periodic spikes from MRI-normal mesial temporal structures were in fact expression of mesial temporal atrophy/sclerosis, as histopathology was not available (these structures were not surgically removed) and mesial temporal atrophy/sclerosis can sometimes defy MRI identification (Wang *et al.*, 2013). Overall, our data further support earlier observations indicating that periodic spikes are

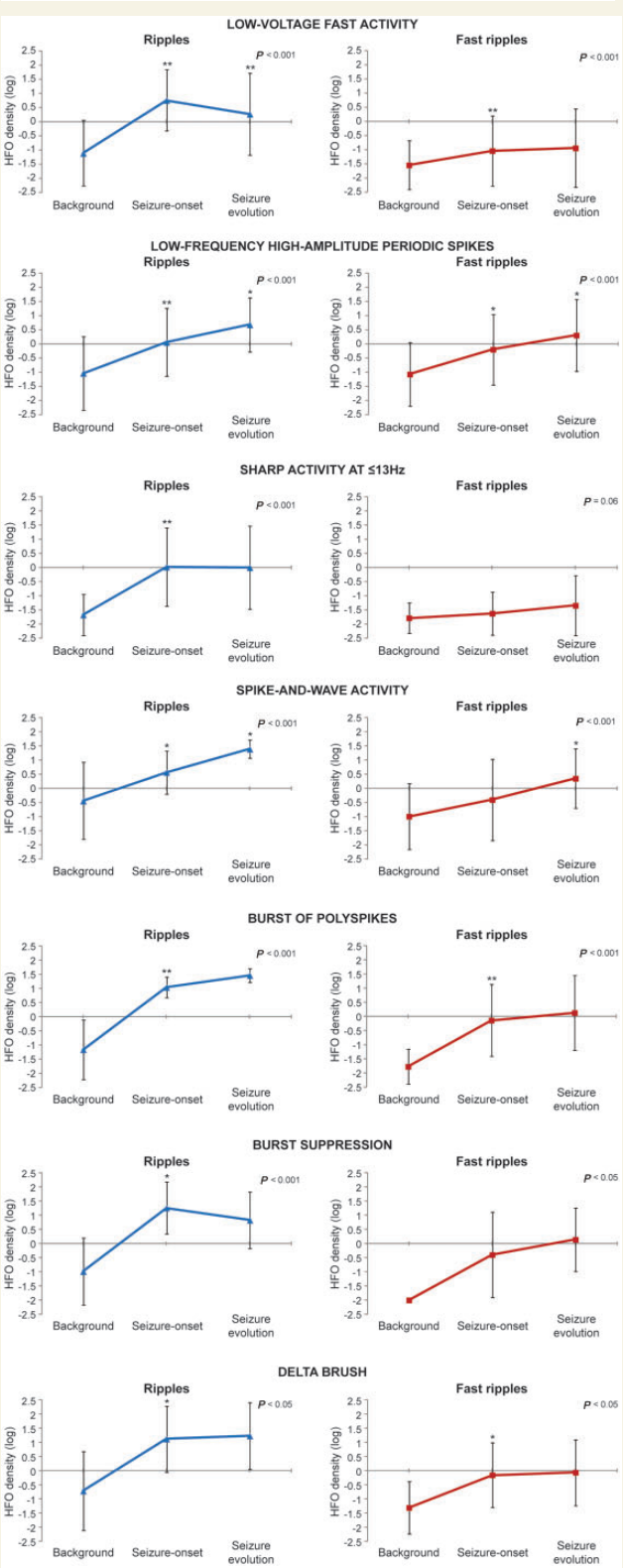

Figure 10 HFO profiles of each of the identified seizure-onset patterns. In each pattern, the HFO density (shown separately for ripples and fast ripples) in electrode contacts located in lesional/peri-lesional tissue and the SOZ increased significantly across the three intracranial EEG sections. This was mainly due to a significant HFO increase at seizure-onset, which was found across all patterns. Values are mean HFO density (log transformed) ± SD (vertical bars). *$P < 0.05$ and **$P < 0.001$, for comparisons between the background and seizure-onset sections and for comparisons between the seizure-onset and seizure evolution sections (repeated-measures ANOVA with Bonferroni correction).

pathognomonic of neuronal loss and gliosis in the mesial temporal lobe, particularly in the hippocampus (Spencer *et al.*, 1992*b*; Park *et al.*, 1996; Spanedda *et al.*, 1997; Velasco *et al.*, 2000; Ogren *et al.*, 2009). Putative pathophysiological mechanisms include enhanced excitation and inhibition, ultimately leading to a hypersynchronous neuronal discharge (Engel, 2013). One has to assume that the mechanisms must be different with other types of seizure-onset pattern.

Delta brush was an uncommon pattern, exclusive to focal cortical dysplasia and occurring in <20% of focal cortical dysplasia seizures. This is an interesting finding because, to the best of our knowledge, it has not been described previously in patients with epilepsy. Before this observation, delta brush had been described in two clinical settings only, being the premiere EEG signature of the premature infant (Clancy *et al.*, 2003) and having been recently found also in patients with anti-*N*-methyl-D-aspartate receptor encephalitis (Johnson *et al.*, 2010; Kirkpatrick *et al.*, 2011; Schmitt *et al.*, 2012). Mechanisms underlying the emergence of delta brush in focal cortical dysplasia are yet to be understood. Intuitively, they would be expected to differ from those involved in the other two clinical settings, as in these cases the pattern is visible on the scalp EEG. However, one of the two patients with focal cortical dysplasia with delta brush also displayed the same pattern at the onset of seizures recorded on scalp EEG (Supplementary Fig. 5). This patient had a larger SOZ [$\text{ratio}_{(\text{SOZ contacts/total contacts})} = 0.175$ versus 0.033]. Aberrant neuronal maturation is considered a prominent feature in focal cortical dysplasia (Najm *et al.*, 2007; Guerrini and Barba, 2010), which might explain why this pathology can exhibit a pattern of activity that normally disappears with complete brain maturation.

We found that, compared with other common patterns, low-voltage fast activity is associated with a more extensive SOZ. Similar observations have been reported previously (Lee *et al.*, 2000; Velasco *et al.*, 2000). In a study in mesial temporal lobe epilepsy, a focal SOZ was found in only one of 18 patients with seizures starting with low-voltage fast activity as opposed to 22 of 35 patients with periodic spikes at seizure-onset ($P < 0.01$) (Velasco *et al.*, 2000). In another study in neocortical epilepsy, a regional SOZ was characteristic of seizures starting with gamma activity, whereas slower frequencies at the onset were associated with a focal SOZ (Lee *et al.*, 2000). It has been postulated that a functional decoupling of distant sites may underlie the emergence of low-voltage fast activity over relatively extensive brain regions (Wendling *et al.*, 2003).

In line with earlier observations (Schiller *et al.*, 1998), we confirmed that propagated activity can also display typical seizure-onset patterns. This was limited to four of the seven patterns, with sharp activity at ⩽ 13 Hz and low-voltage fast activity being the most common seizure-onset patterns found in regions of

spread (Table 2). It should be noted, however, that three patterns not detected in regions of spread (burst of polyspikes, burst suppression and delta brush) were rare and, therefore, it cannot be excluded that there is no pattern that can reliably distinguish seizure-onset from spread. The finding that low-voltage fast activity was detected in regions of spread is intriguing, because such activity is generally regarded as a biomarker of the actual SOZ (Bancaud *et al.*, 1970; Gloor, 1975; Fisher *et al.*, 1992; Lee *et al.*, 2000; Tassi *et al.*, 2002; Wendling *et al.*, 2003; de Curtis and Gnatkovsky, 2009; David *et al.*, 2011) and, potentially, of the epileptogenic zone (Faught *et al.*, 1992; Alarcon *et al.*, 1995; Wetjen *et al.*, 2009). Our observations in this respect are exemplified by Fig. 9, which shows the intracranial EEG correlate of a seizure originating in the left cingulate gyrus with low-voltage fast activity and rapidly propagating to the contralateral region with the same pattern. If the left cingulate gyrus had not been sampled, the SOZ could have been falsely localized to the contralateral hemisphere. Clearly, these findings indicate that interpretative caution should be exerted when an intracranial EEG pattern is used in trying to define the boundaries of the epileptogenic zone. These findings also challenge the concept of a passive propagation from the focus, raising the possibility that several seizures start sequentially, first at the 'early' focus and then at 'later' foci.

Another finding of the present study is that HFOs increase at seizure-onset independently of the type of seizure-onset pattern. This increase was found for ripples and fast ripples in four patterns (low-voltage fast activity, periodic spikes, burst of polyspikes and delta brush), and for ripples only in the remaining three patterns. In the latter group, however, there was also a tendency for fast ripples to increase at seizure onset (Fig. 10), although the change did not reach statistical significance possibly because of sample size limitations. Of note, after seizure-onset, HFOs remained relatively stable in most patterns. Therefore, these findings do not support the suggestion, based on data from animal experiments, that different seizure-onset patterns may carry distinct HFO profiles (Bragin *et al.*, 2005; Lévesque *et al.*, 2012). Instead, the similarities of HFOs changes across different seizure-onset patterns could imply that common mechanisms may be shared by these patterns. Our study, however, only investigated changes in HFO density over three characteristic intracranial EEG sections for each seizure, and it cannot be excluded that other HFO characteristics not evaluated in our analysis, such as amplitude, morphology or duration of individual events, may vary across different patterns.

Assessing the effect of distinct lesions on the emergence of intracranial EEG seizure-onset patterns should take into account potential confounders, such as electrode type and the affected anatomical region. In our study, patterns were not influenced by the type of depth electrodes used in the intracranial EEG investigation; it remains unknown whether differences would have been found if subdural electrodes had been used. Patterns were also not influenced by the anatomical location of the SOZ. Two rare patterns, burst of polyspikes and burst suppression, each shared by two pathologies, were only recorded in the frontal lobe, but numbers are too small to draw any definite conclusion.

Acknowledgements

This manuscript is dedicated to the memory of Dr. Susan Spencer, whose pioneering work in field of EEG and epilepsy has been a continuing inspiration to the authors. The authors are grateful to the staff and technicians at the EEG Department of the Montreal Neurological Institute for their assistance in the study.

Funding

This work was supported by the 'Susan S. Spencer clinical research training fellowship in epilepsy' from the American Brain Foundation, the American Epilepsy Society, and the Epilepsy Foundation (to P.P.); and the Canadian Institutes of Health Research (grant no. MOP-10189).

Supplementary material

Supplementary material is available at *Brain* online.

References

Alarcon G, Binnie CD, Elwes RD, Polkey CE. Power spectrum and intracranial EEG patterns at seizure onset in partial epilepsy. Electroencephalogr Clin Neurophysiol 1995; 94: 326–37.

Bancaud J, Angelergues R, Bernouilli C, Bonis A, Bordas-Ferrer M, Bresson M, et al. Functional stereotaxic exploration (SEEG) of epilepsy. Electroencephalogr Clin Neurophysiol 1970; 28: 85–6.

Bartolomei F, Wendling F, Regis J, Gavaret M, Guye M, Chauvel P. Pre-ictal synchronicity in limbic networks of mesial temporal lobe epilepsy. Epilepsy Res 2004; 61: 89–104.

Bartolomei F, Chauvel P, Wendling F. Epileptogenicity of brain structures in human temporal lobe epilepsy: a quantified study from intracerebral EEG. Brain 2008; 131: 1818–30.

Bénar CG, Chauviere L, Bartolomei F, Wendling F. Pitfalls of high-pass filtering for detecting epileptic oscillations: a technical note on "false" ripples. Clin Neurophysiol 2010; 121: 301–10.

Berg AT, Berkovic SF, Brodie MJ, Buchhalter J, Cross JH, van Emde Boas W, et al. Revised terminology and concepts for organization of seizures and epilepsies: report of the ILAE Commission on Classification and Terminology, 2005-2009. Epilepsia 2010; 51: 676–85.

Blümcke I, Thom M, Aronica E, Armstrong DD, Vinters HV, Palmini A, et al. The clinicopathologic spectrum of focal cortical dysplasias: a consensus classification proposed by an ad hoc Task Force of the ILAE Diagnostic Methods Commission. Epilepsia 2011; 52: 158–74.

Bragin A, Mody I, Wilson CL, Engel J Jr. Local generation of fast ripples in epileptic brain. J Neurosci 2002; 22: 2012–21.

Bragin A, Azizyan A, Almajano J, Wilson CL, Engel J Jr. Analysis of chronic seizure onsets after intrahippocampal kainic acid injection in freely moving rats. Epilepsia 2005; 46: 1592–8.

Bragin A, Azizyan A, Almajano J, Engel J Jr. The cause of the imbalance in the neuronal network leading to seizure activity can be predicted by the electrographic pattern of the seizure onset. J Neurosci 2009; 29: 3660–71.

Clancy RR, Bergqvist AGC, Dlugos DJ. Neonatal electroencephalography. In: Ebersole JS, Pedley TA, editors. Current Practice of Clinical Electroencephalography. 3rd edn. Philadephia: Lippincott Williams & Wilkins; 2003. p. 160–234.

David O, Blauwblomme T, Job AS, Chabardes S, Hoffmann D, Minotti L, et al. Imaging the seizure onset zone with stereo-electroencephalography. Brain 2011; 134: 2898–911.

de Curtis M, Gnatkovsky V. Reevaluating the mechanisms of focal ictogenesis: the role of low-voltage fast activity. Epilepsia 2009; 50: 2514–25.

Dolezalova I, Brazdil M, Hermanova M, Horakova I, Rektor I, Kuba R. Intracranial EEG seizure onset patterns in unilateral temporal lobe epilepsy and their relationship to other variables. Clin Neurophysiol 2013; 124: 1079–88.

Engel J Jr, Van Ness PC, Rasmussen TB, Ojemann LM. Outcome with respect to epileptic seizures. In: Engel J Jr, editor. Surgical treatment of the epilepsies. New York: Raven Press; 1993. p. 609–21.

Engel J Jr. Seizures and epilepsy. 2nd edn. New York: Oxford University Press; 2013.

Faught E, Kuzniecky RI, Hurst DC. Ictal EEG wave forms from epidural electrodes predictive of seizure control after temporal lobectomy. Electroencephalogr Clin Neurophysiol 1992; 83: 229–35.

Fisher RS, Webber WR, Lesser RP, Arroyo S, Uematsu S. High-frequency EEG activity at the start of seizures. J Clin Neurophysiol 1992; 9: 441–8.

Fisher RS, van Emde Boas W, Blume W, Elger C, Genton P, Lee P, et al. Epileptic seizures and epilepsy: definitions proposed by the International League Against Epilepsy (ILAE) and the International Bureau for Epilepsy (IBE). Epilepsia 2005; 46: 470–2.

Galanopoulou AS, Gorter JA, Cepeda C. Finding a better drug for epilepsy: the mTOR pathway as an antiepileptogenic target. Epilepsia 2012; 53: 1119–30.

Gloor P. Contributions of electroencephalography and electrocorticography to the neurosurgical treatment of the epilepsies. In: Purpura D, Penry J, Walter R, editors. Neurosurgical management of the epilepsies. New York: Raven Press; 1975. p. 59–105.

Gnatkovsky V, Librizzi L, Trombin F, de Curtis M. Fast activity at seizure onset is mediated by inhibitory circuits in the entorhinal cortex *in vitro*. Ann Neurol 2008; 64: 674–86.

Guerrini R, Barba C. Malformations of cortical development and aberrant cortical networks: epileptogenesis and functional organization. J Clin Neurophysiol 2010; 27: 372–9.

Jacobs J, Zijlmans M, Zelmann R, Chatillon CE, Hall J, Olivier A, et al. High-frequency electroencephalographic oscillations correlate with outcome of epilepsy surgery. Ann Neurol 2010; 67: 209–20.

Jirsch JD, Urrestarazu E, LeVan P, Olivier A, Dubeau F, Gotman J. High-frequency oscillations during human focal seizures. Brain 2006; 129: 1593–608.

Johnson N, Henry C, Fessler AJ, Dalmau J. Anti-NMDA receptor encephalitis causing prolonged nonconvulsive status epilepticus. Neurology 2010; 75: 1480–2.

Khosravani H, Mehrotra N, Rigby M, Hader WJ, Pinnegar CR, Pillay N, et al. Spatial localization and time-dependant changes of electrographic high frequency oscillations in human temporal lobe epilepsy. Epilepsia 2009; 50: 605–16.

Kirkpatrick MP, Clarke CD, Sonmezturk HH, Abou-Khalil B. Rhythmic delta activity represents a form of nonconvulsive status epilepticus in anti-NMDA receptor antibody encephalitis. Epilepsy Behav 2011; 20: 392–4.

Landis JR, Koch GG. The measurement of observer agreement for categorical data. Biometrics 1977; 33: 159–74.

Lee SA, Spencer DD, Spencer SS. Intracranial EEG seizure-onset patterns in neocortical epilepsy. Epilepsia 2000; 41: 297–307.

Lévesque M, Salami P, Gotman J, Avoli M. Two seizure-onset types reveal specific patterns of high-frequency oscillations in a model of temporal lobe epilepsy. J Neurosci 2012; 32: 13264–72.

Mohanraj R, Brodie MJ. Outcomes in newly diagnosed localization-related epilepsies. Seizure 2005; 14: 318–23.

Najm IM, Tilelli CQ, Oghlakian R. Pathophysiological mechanisms of focal cortical dysplasia: a critical review of human tissue studies and animal models. Epilepsia 2007; 48 (Suppl. 2): 21–32.

Ogren JA, Bragin A, Wilson CL, Hoftman GD, Lin JJ, Dutton RA, et al. Three-dimensional hippocampal atrophy maps distinguish two common temporal lobe seizure-onset patterns. Epilepsia 2009; 50: 1361–70.

Olivier A, Germano IM, Cukiert A, Peters T. Frameless stereotaxy for surgery of the epilepsies: preliminary experience. Technical note. J Neurosurg 1994; 81: 629–33.

Park YD, Murro AM, King DW, Gallagher BB, Smith JR, Yaghmai F. The significance of ictal depth EEG patterns in patients with temporal lobe epilepsy. Electroencephalogr Clin Neurophysiol 1996; 99: 412–5.

Pitkänen A, Kharatishvili I, Karhunen H, Lukasiuk K, Immonen R, Nairismagi J, et al. Epileptogenesis in experimental models. Epilepsia 2007; 48 (Suppl 2): 13–20.

Pitkänen A, Lukasiuk K. Mechanisms of epileptogenesis and potential treatment targets. Lancet Neurol 2011; 10: 173–86.

Schiller Y, Cascino GD, Busacker NE, Sharbrough FW. Characterization and comparison of local onset and remote propagated electrographic seizures recorded with intracranial electrodes. Epilepsia 1998; 39: 380–8.

Schmitt SE, Pargeon K, Frechette ES, Hirsch LJ, Dalmau J, Friedman D. Extreme delta brush: a unique EEG pattern in adults with anti-NMDA receptor encephalitis. Neurology 2012; 79: 1094–100.

Spanedda F, Cendes F, Gotman J. Relations between EEG seizure morphology, interhemispheric spread, and mesial temporal atrophy in bitemporal epilepsy. Epilepsia 1997; 38: 1300–14.

Spencer SS, Guimaraes P, Katz A, Kim J, Spencer D. Morphological patterns of seizures recorded intracranially. Epilepsia 1992a; 33: 537–45.

Spencer SS, Kim J, Spencer DD. Ictal spikes: a marker of specific hippocampal cell loss. Electroencephalogr Clin Neurophysiol 1992b; 83: 104–11.

Tassi L, Colombo N, Garbelli R, Francione S, Lo Russo G, Mai R, et al. Focal cortical dysplasia: neuropathological subtypes, EEG, neuroimaging and surgical outcome. Brain 2002; 125: 1719–32.

Velasco AL, Wilson CL, Babb TL, Engel J Jr. Functional and anatomic correlates of two frequently observed temporal lobe seizure-onset patterns. Neural Plast 2000; 7: 49–63.

Vezzani A. Before epilepsy unfolds: finding the epileptogenesis switch. Nat Med 2012; 18: 1626–7.

Wang ZI, Alexopoulos AV, Jones SE, Jaisani Z, Najm IM, Prayson RA. The pathology of magnetic-resonance-imaging-negative epilepsy. Mod Pathol 2013; 26: 1051–8.

Wendling F, Bartolomei F, Bellanger JJ, Bourien J, Chauvel P. Epileptic fast intracerebral EEG activity: evidence for spatial decorrelation at seizure onset. Brain 2003; 126: 1449–59.

Wennberg R, Arruda F, Quesney LF, Olivier A. Preeminence of extrahippocampal structures in the generation of mesial temporal seizures: evidence from human depth electrode recordings. Epilepsia 2002; 43: 716–26.

Wetjen NM, Marsh WR, Meyer FB, Cascino GD, So E, Britton JW, et al. Intracranial electroencephalography seizure onset patterns and surgical outcomes in nonlesional extratemporal epilepsy. J Neurosurg 2009; 110: 1147–52.

Williamson A, Spencer SS, Spencer DD. Depth electrode studies and intracellular dentate granule cell recordings in temporal lobe epilepsy. Ann Neurol 1995; 38: 778–87.

Zijlmans M, Jacobs J, Zelmann R, Dubeau F, Gotman J. High-frequency oscillations mirror disease activity in patients with epilepsy. Neurology 2009; 72: 979–86.

Zijlmans M, Jacobs J, Kahn YU, Zelmann R, Dubeau F, Gotman J. Ictal and interictal high frequency oscillations in patients with focal epilepsy. Clin Neurophysiol 2011; 122: 664–71.

Zijlmans M, Jiruska P, Zelmann R, Leijten FS, Jefferys JG, Gotman J. High-frequency oscillations as a new biomarker in epilepsy. Ann Neurol 2012; 71: 169–78.